Elastic neutrino-proton scattering*

Ephraim Fischbach, J. Thomas Gruenwald, S. P. Rosen, and Harvey Spivack
Physics Department, Purdue University, West Lafayette, Indiana 47907

Boris Kayser
Physics Division, National Science Foundation, Washington, D. C. 20550

(Received 7 September 1976)

A general analysis of elastic neutrino- and antineutrino-proton scattering is presented which emphasizes the use of these processes as probes of the space-time structure of the weak neutral current. We begin by exhibiting the most general matrix elements in terms of the scalar (S), pseudoscalar (P), tensor (T), vector (V), and axial-vector (A) form factors. These matrix elements are then used to calculate the differential cross sections $d\sigma/dt$ and the proton polarization for incident ν_μ and $\bar{\nu}_\mu$. Based on these results tests are suggested to discriminate between the S,P,T and V,A covariants which respectively flip or preserve the incident neutrino helicity. It is noted that when V, A, and T are all absent from the neutral current, the differential cross sections take the simple form $d\sigma^{\nu,\bar{\nu}}/dt = tf(t)/E_\nu{}^2$, where E_ν is the laboratory energy of the incident neutrinos, t is the square of the momentum transfer, and $f(t)$ is a proton form factor. This observation suggests several ways of discriminating between S,P,T and V,A couplings including a comparison of $d\sigma^\nu/dt$ and $d\sigma^{\bar{\nu}}/dt$, and an examination of the average momentum transfer $\langle t\rangle$. Since some of these tests are subject to the "confusion theorem" (i.e., the ability of S,P,T to mimic V,A), consideration is given to experiments in which the proton polarization is measured. Although such experiments are difficult to perform, the expected effects are strikingly large, and can lead to an unambiguous disentangling of V,A from S,P,T. A discussion is also given of the ν and $\bar{\nu}$ elastic cross sections which, when compared to experiment, suggest that the neutral current is not predominantly S,P.

I. INTRODUCTION

In a recent Letter[1] we examined the data[2,3] on elastic neutrino-proton scattering, $\nu_\mu p \to \nu_\mu p$, from the point of view of discriminating among models of the neutral weak current. Of particular interest was the possibility of probing the space-time structure of the neutral current as characterized by the usual Dirac covariants: vector (V), axial-vector (A), scalar (S), pseudoscalar (P), and tensor (T). We indicated that the data appear to rule out a pure S,P neutral current and we discussed several ways of confirming this conclusion. More recent data[4] on the reaction $\bar{\nu}_\mu p \to \bar{\nu}_\mu p$ have already provided one of the possible confirmations. In this paper we present a discussion of our previous analysis.

The arguments we presented against pure S,P coupling were based on the total elastic rate. Although there is no fundamental theory to fix the scale of the S,P neutral-current interaction, the elastic cross section is constrained by the rate for the inclusive reaction $\nu_\mu p \to \nu_\mu X$. Using the methods of Sakurai and Urrutia,[5] and of Adler and co-workers,[6] to estimate the elastic cross section in terms of the inclusive one, we found that the observed elastic cross section is larger than the estimated one by a factor of approximately 2.

Extrapolating from high-energy inclusive scattering to lower-energy elastic scattering is, of course, a model-dependent procedure. We therefore proposed a series of model-independent tests of the conclusion that the neutral-current interaction is not pure S,P. The simplest of these is the measurement of the cross section for antineutrino-proton elastic scattering: For a pure S,P interaction, the differential cross sections for $\nu_\mu p \to \nu_\mu p$ and $\bar{\nu}_\mu p \to \bar{\nu}_\mu p$ must be precisely equal at the same energy, for all admixtures of S and P, and for all choices of the hadronic form factors. Therefore the observation that $\sigma(\nu_\mu p) \neq \sigma(\bar{\nu}_\mu p)$ immediately excludes a pure S,P interaction.

Other tests include the shape and energy dependence of the $\nu_\mu p$ differential cross section $d\sigma^\nu/dt$, and the polarization of the recoil proton. The shape and energy dependence tests follow from the observation that when V, A, and T are all absent from the neutral current, the differential cross section takes the simple form

$$\frac{d\sigma}{dt} = \frac{tf(t)}{E_\nu{}^2}. \tag{1.1}$$

Here E_ν is the laboratory energy of the incident neutrino, t is the square of the momentum transfer, and $f(t)$ is essentially a proton form factor. From Eq. (1.1) it follows that

(i) if $d\sigma^\nu(t=0)/dt \neq 0$, then at least one of V,A,T is present in the interaction, and

(ii) if $E_\nu{}^2 d\sigma/dt \neq$ constant for a fixed t and any range of E_ν, then again at least one of V, A, or

T must be present. When $E_\nu \gg m$ (the proton mass) and $\sqrt{-t}$, the latter interactions lead to

$$E_\nu^2 \frac{d\sigma^\nu}{dt} \propto E_\nu^2 . \tag{1.2}$$

In our Letter[1] we examined the implications of point (i) for the shape of the t distribution. We concluded that the shape cannot be used to confirm the smallness, or complete absence, of S,P until the range of observable t values is extended from $0.3 \leq |t| \leq 0.9$ (GeV/c)^2 to values at or below $|t| \approx 0.2$ (GeV/c)^2. In the present paper we study the implications of point (i) for the average momentum transfer $\langle t \rangle$. For S,P couplings $\langle t \rangle$ will be "large" because of the vanishing of $d\sigma^{S,P}/dt$ at $t=0$. However, for V,A interactions $\langle t \rangle$ will tend to be "small" because $d\sigma^{V,A}/dt$ is largest in the forward direction and decreases as $|t|$ increases. Given reasonably shaped form factors, the value of $\langle t \rangle$ must lie within definite bounds for each of these classes of interaction, irrespective of the detailed S,P or V,A admixture.

The test comparing neutrino and antineutrino differential cross sections is based on the observation that

(iii) $d\sigma^\nu/dt \neq d\sigma^{\bar\nu}/dt$ implies that the interaction is neither pure V, nor pure A, nor pure T, nor any combination of only S and P. Besides excluding S,P this comparison is also an important test of models which have a pure V neutral current.[7]

The polarization of the outgoing proton, should it become measurable, could also be a very useful tool in analyzing the interaction. To see this, consider angular momentum conservation for forward scattering: If the polarization of the scattered proton is anything other than -100% with respect to the beam direction, then some helicity-conserving V or A must be present in the interaction. We shall present detailed calculations which show that polarization measurements away from the forward direction can be similarly useful.

Besides illuminating the general character of the interaction, νp scattering will, of course, help determine the finer details of the space-time structure (such as the Weinberg angle) and the isospin structure of the hadronic neutral current.

The plan of this paper is as follows: The kinematics of νp scattering is described in Sec. II and the most general form of the matrix element, including hadronic form factors, is discussed in Sec. III. Section IV contains the calculation of the average momentum transfer $\langle t \rangle$ for different interactions and different incident neutrino spectra. Polarization is considered in Sec. V, and results for the total cross section [integrated from $|t| = 0.3$ (GeV/c)^2 to $|t| = 0.9$ (GeV/c)^2] for various theoretical models are presented in Sec. VI. Detailed formulas for the νp differential cross section and the polarization of the outgoing proton are given in the Appendix.

II. KINEMATICS

The kinematics for the elastic scattering $\nu_\mu(Q) + p(P) \to \nu_\mu(Q') + p(P')$ is shown in the laboratory frame in Fig. 1. Owing to experimental cuts, only protons with a laboratory energy in excess of some minimum value $P_0'^{\min}$ will be observed, and so the accessible range of momentum transfer for a fixed value of s is

$$t_1 < |t| < t_2(s) , \tag{2.1a}$$

$$t_1 = 2m(P_0'^{\min} - m) , \tag{2.1b}$$

$$t_2(s) = (s - m^2)^2/s , \tag{2.1c}$$

where m is the proton mass. The kinematic range defined by Eqs. (2.1) corresponds to the shaded region in Fig. 1. In practice, of course, the incident neutrino beam is not monoenergetic but is described instead by some flux distribution function $\Phi(Q_0)$ such as that shown for the Argonne (ANL) spectrum[8] in Fig. 2 and Table I, and the Brookhaven (BNL) spectrum[9] in Fig. 3 and Table II. However, for each elastic scattering event, the entire kinematics can be reconstructed, given a knowledge of the proton 3-momentum $\vec{P}'$ and the incident beam direction $\hat{Q}$. In particular, the incident neutrino energy Q_0 is given by

$$Q_0 = \frac{(P_0' - m)^2 - |\vec{P}'|^2}{2(P_0' - P_z' - m)} , \tag{2.2}$$

where the neutrino-beam direction has been taken

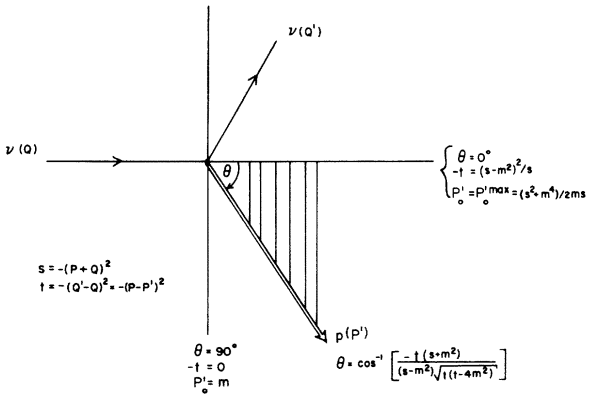

FIG. 1. Kinematics for the elastic scattering process $\nu(Q) + p(P) \to \nu(Q') + p(P')$ in the laboratory frame, where the quantities in parentheses denote the 4-momenta of the particles. The shaded region indicates the accessible values of the kinematic variables for an experiment in which the only protons detected are those whose energy P_0' is in excess of some minimum value $P_0'^{\min} = m - \frac{1}{2}t^{\min}/m$.

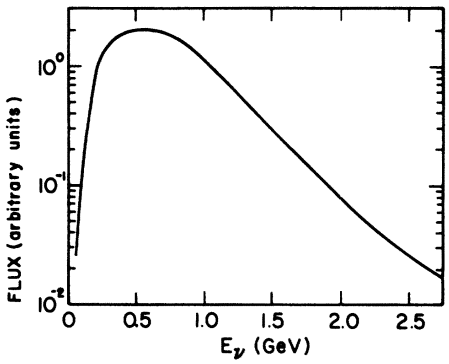

FIG. 2. The Argonne neutrino-flux distribution. For present purposes the absolute normalization of the neutrino flux is immaterial.

to be along the z axis. Given Q_0 and $\vec{P}'$ we can then deduce

$$s = m(m + 2Q_0) \tag{2.3a}$$

and

$$-t = 2m(P_0' - m) \tag{2.3b}$$

for each scattering event.

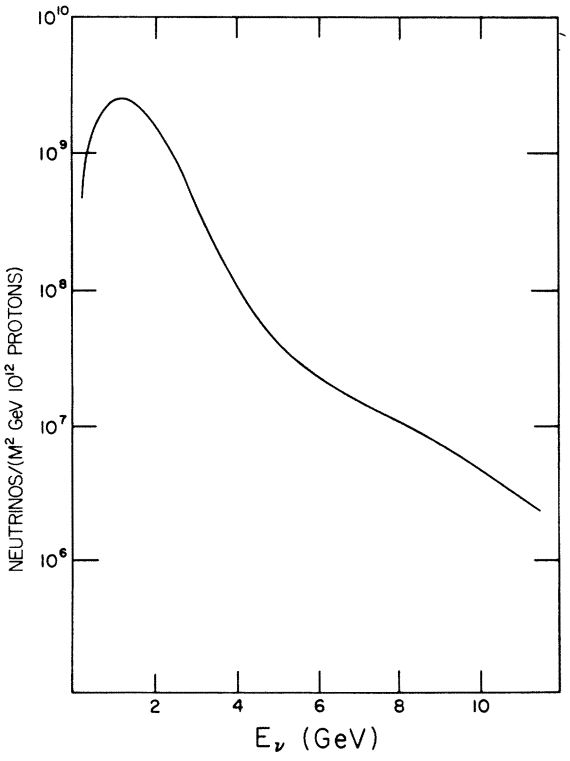

FIG. 3. The Brookhaven neutrino-flux distribution.

TABLE I. The Argonne neutrino spectrum. Q_0 is the neutrino energy in GeV and $\Phi(Q_0)$ is the corresponding flux in arbitrary units.

Q_0	$\Phi(Q_0)$	Q_0	$\Phi(Q_0)$
0.2	0.7400	3.1	0.0137
0.3	1.4864	3.2	0.0132
0.4	1.7477	3.3	0.0127
0.5	1.8893	3.4	0.0122
0.6	1.9350	3.5	0.0117
0.7	1.8742	3.6	0.0113
0.8	1.6796	3.7	0.0109
0.9	1.3864	3.8	0.0106
1.0	1.1063	3.9	0.0102
1.1	0.8546	4.0	0.0099
1.2	0.6437	4.1	0.0095
1.3	0.4964	4.2	0.0091
1.4	0.3856	4.3	0.0087
1.5	0.2907	4.4	0.0083
1.6	0.2225	4.5	0.0080
1.7	0.1718	4.6	0.0076
1.8	0.1303	4.7	0.0072
1.9	0.0972	4.8	0.0069
2.0	0.0727	4.9	0.0065
2.1	0.0577	5.0	0.0062
2.2	0.0468	5.1	0.0057
2.3	0.0386	5.2	0.0053
2.4	0.0322	5.3	0.0049
2.5	0.0267	5.4	0.0045
2.6	0.0233	5.5	0.0042
2.7	0.0205	5.6	0.0039
2.8	0.0180	5.7	0.0037
2.9	0.0160	5.8	0.0034
3.0	0.0145	5.9	0.0032
		6.0	0.0030

TABLE II. The Brookhaven neutrino spectrum. Q_0 is the neutrino energy in GeV and $\Phi(Q_0)$ is the corresponding flux in arbitrary units.

Q_0	$\Phi(Q_0)$	Q_0	$\Phi(Q_0)$
0.25	0.8200	5.00	0.0410
0.50	1.6000	5.25	0.0330
0.75	2.0000	5.50	0.0290
1.00	2.3000	5.75	0.0250
1.25	2.3000	6.00	0.0220
1.50	2.2000	6.25	0.0200
1.75	1.8000	6.50	0.0180
2.00	1.6000	6.75	0.0160
2.25	1.1000	7.00	0.0150
2.50	0.9000	7.25	0.0140
2.75	0.6400	7.50	0.0130
3.00	0.4300	7.75	0.0120
3.25	0.2900	8.00	0.0110
3.50	0.2000	8.25	0.0100
3.75	0.1500	8.50	0.0090
4.00	0.1100	8.75	0.0082
4.25	0.0820	9.00	0.0074
4.50	0.0640	9.25	0.0067
4.75	0.0470	9.50	0.0061
		9.75	0.0055

III. MATRIX ELEMENT FOR $\nu_\mu\ (\bar{\nu}_\mu)+p\to\nu_\mu\ (\bar{\nu}_\mu)+p$

A. General considerations

Allowing the neutrino-proton interaction to have its most general point coupling form, we can write the matrix element $\mathcal{T}$ for elastic neutrino-proton scattering in the form

$$\mathcal{T}=\frac{2G}{\sqrt{2}}\sum_{i=S,P,V,A,T}\bar{u}(Q')\Gamma_i u(Q)\mathfrak{M}^i(P,P')\,. \tag{3.1}$$

Here $u(Q)$ and $\bar{u}(Q')$ are the incoming and outgoing neutrino wave functions, respectively, and we have $\Gamma_S=1$, $\Gamma_P=i\gamma_5$, $\Gamma_V=i\gamma_\lambda$, $\Gamma_A=i\gamma_\lambda\gamma_5$, and $\Gamma_T=\sigma_{\lambda\mu}$. For incident antineutrinos $u(Q)\to v(Q')$ and $\bar{u}(Q')\to\bar{v}(Q)$. The (Hermitian) hadronic currents $\mathfrak{M}^i(P,P')$ are given by

$$\mathfrak{M}^S(P,P')=\bar{u}(P')[C^S(t)+i\gamma_5 D^S(t)]u(P)\,, \tag{3.2a}$$

$$\mathfrak{M}^P(P,P')=\bar{u}(P')[i\gamma_5 C^P(t)+D^P(t)]u(P)\,, \tag{3.2b}$$

$$\mathfrak{M}^V_\lambda(P,P')=i\bar{u}(P')\left\{\gamma_\lambda[C_1^V(t)+\gamma_5 D_1^V(t)]+\frac{\sigma_{\lambda\alpha}q_\alpha}{2m}[C_2^V(t)+\gamma_5 D_2^V(t)]+\frac{iq_\lambda}{2m}[C_3^V(t)+\gamma_5 D_3^V(t)]\right\}u(P)\,, \tag{3.2c}$$

$$\mathfrak{M}^A_\lambda(P,P')=i\bar{u}(P')\left\{\gamma_\lambda\gamma_5[C_1^A(t)+\gamma_5 D_1^A(t)]+\frac{\sigma_{\lambda\alpha}q_\alpha}{2m}\gamma_5[C_2^A(t)+\gamma_5 D_2^A(t)]+\frac{iq_\lambda\gamma_5}{2m}[C_3^A(t)+\gamma_5 D_3^A(t)]\right\}u(P)\,, \tag{3.2d}$$

$$\mathfrak{M}^T_{\lambda\mu}(P,P')=\bar{u}(P')\sum_{a=1}^{4}[\Gamma^a_{\lambda\mu}C_a^T(t)+\tfrac{1}{2}i\epsilon_{\lambda\mu\alpha\beta}\Gamma^a_{\alpha\beta}D_a^T(t)]u(P)\,, \tag{3.2e}$$

$$\Gamma^1_{\lambda\mu}=\sigma_{\lambda\mu}=(\gamma_\lambda\gamma_\mu-\gamma_\mu\gamma_\lambda)/2i,\quad \Gamma^2_{\lambda\mu}=(\gamma_\lambda q_\mu-\gamma_\mu q_\lambda)/m,\quad \Gamma^3_{\lambda\mu}=i(\gamma_\lambda k_\mu-\gamma_\mu k_\lambda)/m,$$

$$\Gamma^4_{\lambda\mu}=i(q_\lambda k_\mu-q_\mu k_\lambda)/m^2,\quad q=P-P',\quad k=P+P',\quad t=-q^2\,.$$

$C^i(t)$ and $D^i(t)$ are defined to be real and dimensionless, and we have written the hadronic currents in such a way that, for each of the five possible couplings, the terms proportional to $D^i(t)$ incorporate the effects of a possible parity violation. If time-reversal invariance is assumed then for S, P, and T

$$\begin{aligned}&D^S=D^P=0\,,\\ &C_3^T=D_1^T=D_2^T=D_4^T=0\,,\end{aligned} \tag{3.3}$$

and if one assumes in addition that second-class currents are absent then

$$D_3^T=0\,. \tag{3.4}$$

Using the Dirac equation we further note that the terms proportional to q_λ make no contribution when multiplied by the leptonic current.

We have written the matrix element in Eqs. (3.1) and (3.2) in a seemingly complicated form in order to emphasize the point that parity violation in $\nu_\mu p$ scattering requires that some of the form factors $D^i(t)$ be different from zero. For the S, P, and T couplings this in turn requires a violation of time-reversal invariance (assuming that second-class currents are absent) as can be seen from Eqs. (3.3) and (3.4). However, when we specialize to the case of incident left-handed neutrinos or right-handed antineutrinos, such as would be the case for conventional neutrino beams produced via the charged-current interactions, the matrix elements in Eqs. (3.1) and (3.2) can be considerably simplified. For $\nu=\nu_L$ we replace $u(Q)$ by $\frac{1}{2}(1+\gamma_5)u(Q)$ in which case the resulting matrix element $\mathcal{T}_L$ can be written in the form

$$\begin{aligned}\mathcal{T}_L=\frac{2G}{\sqrt{2}}\Big\{&\bar{u}(Q')\tfrac{1}{2}(1+\gamma_5)u(Q)\bar{u}(P')[S(t)+\gamma_5 P(t)]u(P)\\ &+i\bar{u}(Q')\gamma_\lambda\tfrac{1}{2}(1+\gamma_5)u(Q)i\bar{u}(P')\left[\gamma_\lambda F_1(t)+\frac{\sigma_{\lambda\alpha}q_\alpha}{2m}F_2(t)+\gamma_\lambda\gamma_5 G_1(t)+\frac{\sigma_{\lambda\alpha}q_\alpha}{2m}\gamma_5 G_2(t)\right]u(P)\\ &+\bar{u}(Q')\sigma_{\lambda\mu}\tfrac{1}{2}(1+\gamma_5)u(Q)\bar{u}(P')\left(\sum_{a=1}^{4}\Gamma^a_{\lambda\mu}T_a(t)\right)u(P)\Big\}\,,\end{aligned} \tag{3.5a}$$

$$S(t)=C^S(t)+iD^P(t),\quad P(t)=-C^P(t)+iD^S(t)\,, \tag{3.5b}$$

$$F_1(t)=C_1^V(t)+D_1^A(t),\quad F_2(t)=C_2^V(t)+D_2^A(t)\,, \tag{3.5c}$$

$$G_1(t)=C_1^A(t)+D_1^V(t),\quad G_2(t)=C_2^A(t)+D_2^V(t)\,, \tag{3.5d}$$

$$T_a(t) = C_a^T(t) - iD_a^T(t)\,. \tag{3.5e}$$

Although the S, P, V, and A contributions in Eqs. (3.5) can be written down by inspection using Eqs. (3.2), the T contribution requires the use of some additional identities such as

$$\sigma_{\lambda\mu}\gamma_5 = -\tfrac{1}{2}\epsilon_{\lambda\mu\alpha\beta}\sigma_{\alpha\beta}\,, \tag{3.6a}$$

$$\sigma_{\lambda\mu} = -\tfrac{1}{2}\epsilon_{\lambda\mu\alpha\beta}\sigma_{\alpha\beta}\gamma_5\,, \tag{3.6b}$$

$$\bar\psi_1\sigma_{\mu\nu}(1\pm\gamma_5)\psi_2\bar\psi_3\sigma_{\mu\nu}(a+b\gamma_5)\psi_4 = \tfrac{1}{2}(a\pm b)\bar\psi_1\sigma_{\mu\nu}(1\pm\gamma_5)\psi_2\bar\psi_3\sigma_{\mu\nu}(1\pm\gamma_5)\psi_4\,, \tag{3.6c}$$

which serve to eliminate the terms proportional to $\epsilon_{\lambda\mu\alpha\beta}\Gamma^a_{\alpha\beta}$ in favor of $\Gamma^a_{\lambda\mu}$.

For incident right-handed antineutrinos, $\bar\nu_R$, the matrix element $\mathcal{T}_R$ is obtained by substituting $\bar v(Q) \to \bar v(Q)\frac{1}{2}(1-\gamma_5)$ giving

$$\begin{aligned}\mathcal{T}_R = \frac{2G}{\sqrt2}\Big\{&\bar v(Q)\tfrac{1}{2}(1-\gamma_5)v(Q')\bar u(P')[S^*(t) - \gamma_5 P^*(t)]u(P)\\ &+ i\bar v(Q)\tfrac{1}{2}(1-\gamma_5)\gamma_\lambda v(Q')i\bar u(P')\Big[\gamma_\lambda F_1(t) + \frac{\sigma_{\lambda\alpha}q_\alpha}{2m}F_2(t) + \gamma_\lambda\gamma_5 G_1(t) + \frac{\sigma_{\lambda\alpha}q_\alpha}{2m}\gamma_5 G_2(t)\Big]u(P)\\ &+ \bar v(Q)\tfrac{1}{2}(1-\gamma_5)\sigma_{\lambda\mu}v(Q')\bar u(P')\Big[\sum_{a=1}^{4}\Gamma^a_{\lambda\mu}T_a^*(t)\Big]u(P)\Big\}\,.\end{aligned} \tag{3.7}$$

Given the matrix elements in Eqs. (3.5) and (3.7), we can calculate the differential cross sections $d\sigma(s,t)/dt$ for incident ν_L and $\bar\nu_R$ as well as the corresponding longitudinal proton polarizations $\mathcal{P}^{\nu,\bar\nu}$. The results are given in the Appendix. We see from Eq. (A1) that $d\sigma(s,t)/dt$ vanishes at $t=0$ for pure S and P couplings, but not for V, A, or T. This observation forms the basis of our attempt to distinguish between S,P on the one hand, and V,A on the other through the shape of the t distribution and momentum transfer $\langle t\rangle$.

We turn next to the high-energy behavior of $d\sigma(s)/dt$. In the limit $s \gg m^2, t$ we find from Eq. (A1) that for both ν and $\bar\nu$

$$\begin{aligned} &d\sigma(s)/dt \propto \text{const} \quad V,A,T\,,\\ &d\sigma(s)/dt \propto 1/s^2 \quad S,P\,.\end{aligned} \tag{3.8}$$

Hence, if $d\sigma(s)/dt$ falls with increasing s the neutrino helicity is definitely flipping. On the other hand, if $d\sigma(s)/dt$ is a constant for large s, the neutrino helicity may or may not be flipping. This is a manifestation of the "confusion theorem,"[10] and can be understood by noting that the tensor interaction involves antisymmetric neutrino and hadron tensors, and corresponds, like V and A, to spin-*one* exchange.

B. Comparison of νp and $\bar\nu p$

We now discuss the relations between the ν and $\bar\nu$ differential cross sections as given by Eq. (A1). We note that for each of the covariants S,P,T,V,A *taken separately* $d\sigma^\nu/dt = d\sigma^{\bar\nu}/dt$. This is trivially true for the S and P covariants which contain no interference terms which can change sign. For the V,A covariants the difference between the ν and $\bar\nu$ interactions appears, as is well known, only through the V,A interference term. For T this statement is a bit less obvious since the hadronic matrix element in Eq. (3.2e) contains terms which transform oppositely under parity, and whose interference terms might thus be expected to distinguish between ν and $\bar\nu$ in analogy to the V,A case. From Eqs. (3.5a) and (3.7) we note that the difference between the ν and $\bar\nu$ matrix elements arises from both the leptonic factors

$$L^\nu_{\lambda\mu}(Q,Q') = \bar u(Q')\sigma_{\lambda\mu}\tfrac{1}{2}(1+\gamma_5)u(Q)\,, \tag{3.9a}$$

$$L^{\bar\nu}_{\lambda\mu}(Q,Q') = \bar v(Q)\tfrac{1}{2}(1-\gamma_5)\sigma_{\lambda\mu}v(Q')\,, \tag{3.9b}$$

and from the replacement of $T_a(t)$ in the hadronic factors $H^\nu_{\lambda\mu}(P,P')$ by $T_a^*(t)$ in $H^{\bar\nu}_{\lambda\mu}(P,P')$. When the squares of the corresponding tensor matrix element, $|\mathcal{T}^T(\nu)|^2$ and $|\mathcal{T}^T(\bar\nu)|^2$, are computed, the leptonic factors are seen, after some manipulation, to be identical:

$$|\mathcal{T}^T(\nu,\bar\nu)|^2 = L^{\nu,\bar\nu}_{\lambda\mu\,\alpha\beta}(Q,Q')H^{\nu,\bar\nu}_{\lambda\mu\,\alpha\beta}(P,P')\,, \tag{3.10a}$$

$$\begin{aligned}L^\nu_{\lambda\mu\,\alpha\beta}(Q,Q') &= \mathrm{Tr}(L^\nu_{\lambda\mu}L^{\nu*}_{\alpha\beta})\\ &\propto \mathrm{Tr}(\sigma_{\lambda\mu}\gamma\cdot Q\sigma_{\alpha\beta}\gamma\cdot Q')\,,\end{aligned} \tag{3.10b}$$

$$\begin{aligned}L^{\bar\nu}_{\lambda\mu\,\alpha\beta}(Q,Q') &= \mathrm{Tr}(L^{\bar\nu}_{\lambda\mu}L^{\bar\nu*}_{\alpha\beta})\\ &\propto \mathrm{Tr}(\sigma_{\lambda\mu}\gamma^\circ Q'\sigma_{\alpha\beta}\gamma^\circ Q)\,.\end{aligned} \tag{3.10c}$$

Thus the difference between the ν and $\bar\nu$ differential cross sections arises solely from the replacement of $T_a(t)$ by $T_a^*(t)$ in going from ν to $\bar\nu$. Using the fact that the covariants $\Gamma^a_{\lambda\mu}$ in Eq. (3.2e) are Hermitian, one can then show that $H^\nu_{\lambda\mu\,\alpha\beta} = H^{\bar\nu}_{\lambda\mu\,\alpha\beta}$, and hence that $d\sigma^\nu/dt = d\sigma^{\bar\nu}/dt$ for the tensor matrix element.

C. Form-factor models

In the preceding subsections we considered the phenomenological properties of the $\nu p \to \nu p$ and $\bar{\nu} p \to \bar{\nu} p$ matrix elements without reference to specific models of the various form factors. Our purpose was to point out the kinematic differences between the helicity-flipping S,P covariants and the helicity-preserving V,A covariants, such as the behavior of the respective differential cross sections at $t=0$. However, detailed experimental results will depend on the normalization and shape of the hadronic form factors. Hence some understanding of the expected behavior of these form factors is necessary. Since observed quantities do depend on form factors, one can use the data not only to distinguish between V,A and S,T,P covariants but also as a test of different models of the V,A interaction, should the neutral current turn out to be helicity-preserving. Thus, form-factor considerations at once complicate the problem of distinguishing between V,A and S,T,P and at the same time make it possible to test different detailed theories of the neutral current.

We begin with the V,A interaction, which has been the focus of considerable attention in recent years. In most theories the V,A neutral current $J_\lambda^N(x)$ is related in one way or another to the known electromagnetic and weak currents $J_\lambda^\gamma(x)$ and $J_\lambda^+(x)$, respectively, whose matrix elements are given by

$$\langle P'|[J_\lambda^\gamma(0)=\mathfrak{F}_\lambda^3(0)+3^{-1/2}\mathfrak{F}_\lambda^8(0)]|P\rangle = i\bar{u}(P')\left[\gamma_\lambda F_1^\gamma(t)+\frac{\sigma_{\lambda\alpha}q_\alpha}{2m}F_2^\gamma(t)\right]u(P)\,, \tag{3.11}$$

$$\langle P'|[J_\lambda^+(0)=\mathfrak{F}_\lambda^{1+i2}(0)+\mathfrak{F}_{5\lambda}^{1+i2}(0)]|P\rangle = i\bar{u}(P')\left[\gamma_\lambda F_1^+(t)+\frac{\sigma_{\lambda\alpha}q_\alpha}{2m}F_2^+(t)+\gamma_\lambda\gamma_5 G_A^+(t)+\frac{iq_\lambda}{2m}\gamma_5 G_P^+(t)\right]u(P)\,. \tag{3.12}$$

In Eqs. (3.11) and (3.12) $\mathfrak{F}_\lambda$ and $\mathfrak{F}_{5\lambda}$ are the usual octet vector and axial-vector currents which satisfy the standard SU(3)⊗SU(3) equal-time commutation relations. The relevant electromagnetic and weak form factors are given at $t=0$ by

$$\begin{aligned} &F_1^\gamma(0)=1\,,\quad F_2^\gamma(0)=\mu_p=1.79\,,\\ &F_1^+(0)=1\,,\quad F_2^+(0)=\mu_p-\mu_n=1.79+1.91=3.70\,,\\ &G_A^+(0)=1.25\pm0.09\,. \end{aligned} \tag{3.13}$$

In Eq. (3.13) μ_p and μ_n are the anomalous magnetic moments of the proton and neutron, respectively. As noted previously the term proportional to $G_P^+(t)$ makes no contribution to elastic νp or $\bar{\nu} p$ scattering. Since the axial-vector current thus depends on a single overall normalization $G_A^+(0)$, $\langle t\rangle$ will actually be independent of $G_A^+(0)$ when the neutral current is a first-class axial-vector current, which is one of the cases considered in Sec. IV below.

One of the most popular models of the neutral current is the so-called Weinberg-Salam (WS) model[11] in which $J_\lambda^N(y)$ is given by

$$\begin{aligned} J_\lambda^N(y)=&\mathfrak{F}_\lambda^3(y)+\mathfrak{F}_{5\lambda}^3(y)-2\sin^2\theta_W J_\lambda^\gamma(y)\\ &+\Delta J_\lambda(y)\,, \end{aligned} \tag{3.14}$$

where θ_W is the Weinberg angle, and $\Delta J_\lambda(y)$ is a $V-A$ strangeness- and charm-containing current which is conventionally assumed to have only a weak coupling to ordinary low-mass hadron states. We will consequently set $\Delta J_\lambda=0$ in our calculations for the WS model. Combining Eqs. (3.11)–(3.14) we see that the form factors $F_1(0)$, $F_2(0)$, and $G_1(0)$ appearing in Eqs. (3.5), (3.7), and (A1) are given in the WS model by

$$F_1(0)=\tfrac{1}{2}(1-4x)\,, \tag{3.15a}$$

$$F_2(0)=\tfrac{1}{2}(\mu_p-\mu_n)-2x\mu_p=1.85-3.59x\,, \tag{3.15b}$$

$$G_1(0)=\tfrac{1}{2}G_A^+(0)=0.63\,, \tag{3.15c}$$

where we have defined $x=\sin^2\theta_W$. The presently favored value is[12] $x\simeq 0.35$. In addition to the WS model and the pure axial-vector current model we have also considered a model in which $J_\lambda^N(y)$ is given by

$$J_\lambda^N(y)=\mathfrak{F}_\lambda^8(y)\,, \tag{3.16}$$

i.e., the neutral current is a pure vector isoscalar. In this case $G_1=0$, and $F_1(0)$ and $F_2(0)$ are given by

$$F_1(0)=\tfrac{1}{2}\,, \tag{3.17a}$$

$$F_2(0)=\tfrac{1}{2}(\mu_p+\mu_n)=-0.06\,. \tag{3.17b}$$

In addition to ascertaining the values of the form factors F_1, F_2, and G_1 at $t=0$, we must also specify their respective t dependences. On the basis of the usual vector-dominance arguments we can presume that F_1, F_2, and G_1 have the same t dependence as the corresponding form factors in the charged-current case. We will thus assume that

$$\frac{F_1(t)}{F_1(0)}=\frac{F_2(t)}{F_2(0)}=\frac{G_1(t)}{G_1(0)}=\frac{1}{(1-t/\Lambda^2)^2}\,, \tag{3.18}$$

with $\Lambda=0.9m$. We shall see in Sec. IV that small variations in Λ produce correspondingly small changes in $\langle t\rangle$.

We turn next to the helicity-flipping S,P,T couplings. Since the very existence of these couplings is yet to be demonstrated, we have treated the corresponding form factors at $t=0$ as arbitrary parameters which we allow to assume all possible values. Should measurements of $\langle t\rangle$ indicate the presence of S,P,T couplings, then a choice among various models of these form factors can be made, as in the case of the V,A couplings, given a precise knowledge of $\langle t\rangle$. Models of the S,P,T form factors have been considered recently by Adler *et al.*[6]

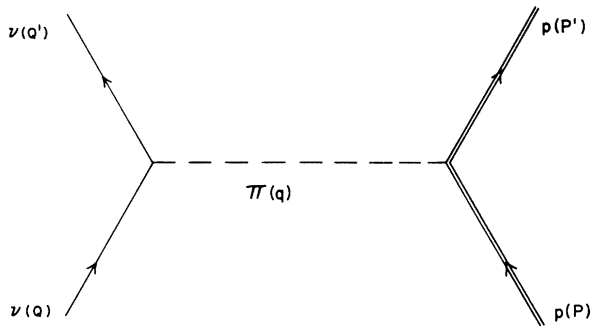

FIG. 4. Pion-pole contribution to the pseudoscalar form factor $P(t)$ in Eq. (3.5).

IV. CALCULATION OF $\langle t\rangle$

As we have noted, $d\sigma/dt$ vanishes at $t=0$ for the S,P couplings, but not for V,A, or T. This can be understood by noting that in the S,P case

$$|\mathcal{T}_{L,R}|^2 \propto |\bar{u}(Q')u(Q)|^2 \propto Q\cdot Q' = t/2 .$$

This behavior of $d\sigma^{S,P}/dt$ is obviously independent of the details of the proton form factors and can, in principle, be used to test for the presence of S,P couplings in a relatively model-independent way. In practice, since the region near $t=0$ is inaccessible experimentally, one must apply this test by studying the shape of the t distribution for $|t| \lesssim 0.2$ (GeV/c)^2, as discussed in the Introduction, or by determining $\langle t\rangle$ in an experiment sensitive to t values not much bigger than this.

Before turning to the detailed calculation of $\langle t\rangle$ we note that since $\langle t\rangle$ is completely determined by $d\sigma/dt$ and the experimental cuts, a complete experimental determination of the differential cross section would make a study of $\langle t\rangle$ unnecessary. However, given the limited data which are presently available, an analysis of $\langle t\rangle$ is very worthwhile for the following reasons: Firstly, $\langle t\rangle$ is insensitive to experimental errors in determining the overall scale of $d\sigma/dt$ and, secondly, because fairly rigorous statements can be made regarding the values of $\langle t\rangle$ that are allowed by various coupling types such as V,A or S,P. Hence $\langle t\rangle$ provides a quick check of whether a given experiment is consistent with a specific coupling.

To see how sensitive $\langle t\rangle$ is to the nature of the interaction, we assume that the form factors appearing in $d\sigma/dt$ have a common t dependence of the form $(1-t/\Lambda^2)^{-2}$ characterized by an as yet unspecified mass Λ. For $P(t)$, which can be dominated by the pion-pole contribution shown in Fig. 4 if the pseudoscalar current transforms as an isovector, we will assume in addition that $P(t)$ may have the form

$$P(t) = \frac{P(0)}{1-t/m_\pi^2} . \tag{4.1}$$

The differential cross sections $d\sigma^\pm/dt$ corresponding to $+=V,A$ and $-=S,P,T$ can then be expressed in the form

$$\frac{d\sigma^\pm}{dt}(s,t) = \frac{-G^2}{8\pi}\frac{1}{(s-m^2)^2} \times \sum_{n=0}^{4} R_n^\pm(s)\frac{t^n}{(1-t/\Lambda^2)^4} , \tag{4.2}$$

where the coefficients $R_n^\pm(s)$ can be read off directly from Eqs. (A3). For the terms proportional to $P(t)$ we substitute $(1-t/m_\pi^2)$ for $(1-t/\Lambda^2)^{-2}$ if pion dominance is assumed. From Eqs. (4.1) and (4.2) we see that the averages $\langle t^\pm(s)\rangle$ derived from $d\sigma^\pm/dt$ can be written as

$$\langle t^\pm(s)\rangle = \frac{\sum_n R_n^\pm(s) I_{n+1}(t_1,t_2)}{\sum_n R_n^\pm(s) I_n(t_1,t_2)} , \tag{4.3}$$

where we have defined

$$I_n(t_1,t_2) = \int_{t_1}^{t_2} dt \frac{t^n}{(1-t/\Lambda^2)^4} . \tag{4.4}$$

For the pion-pole contribution we require in addition the integrals $J_n(t_1,t_2)$ and $K_n(t_1,t_2)$, where

$$J_n(t_1,t_2) = \int_{t_1}^{t_2} dt \frac{t^n}{(1-t/m_\pi^2)^2} , \tag{4.5a}$$

$$K_n(t_1,t_2) = \int_{t_1}^{t_2} dt \frac{t^n}{(1-t/\Lambda^2)^2(1-t/m_\pi^2)} . \tag{4.5b}$$

Although neutrino beams are not monoenergetic, it is nonetheless of interest to examine $\langle t^\pm(s)\rangle$ for a fixed value of s before confronting the problems associated with the neutrino spectrum. Figure 5 compares $\langle t^-\rangle \equiv \langle t^{S,P}\rangle$ and $\langle t^+\rangle \equiv \langle t^{V,A}\rangle$ at an incident neutrino energy $Q_0 = m/2$, which is near the peak in the Argonne flux distribution. For the V,A matrix element we use the previously described Weinberg-Salam model parametrized by $x=\sin^2\theta_W$, and we have taken $\Lambda = m$ for illustrative purposes.

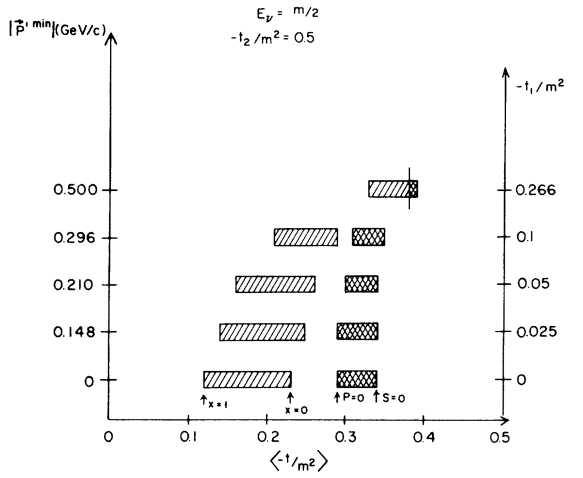

FIG. 5. $\langle -t/m^2 \rangle$ as a function of t_1 for a monoenergetic neutrino beam with $E_\nu \equiv Q_0 = m/2$ (corresponding to a maximum momentum transfer $-t_2 = 0.5m^2$). For each value of the minimum momentum transfer t_1 (or the proton momentum $|\vec{P}'|$) the doubly hatched region gives the range of values of $\langle -t/m^2 \rangle$ corresponding to an arbitrary admixture of the form factors $S(t)$ and $P(t)$. The arrows labeled $S=0$ and $P=0$ denote the extreme cases $S(t)=0$ and $P(t)=0$, respectively. The singly hatched band gives the corresponding predictions for the Weinberg-Salam model of the V,A current discussed in the text, with $x=\sin^2\theta_W$. Note that the distinction between V,A and S,P increases as $|t_1|$ decreases. Inclusion of a T contribution would blur this distinction. All form factors are assumed for simplicity to have the dipole t dependence of Eq. (3.18) with $\Lambda = m$.

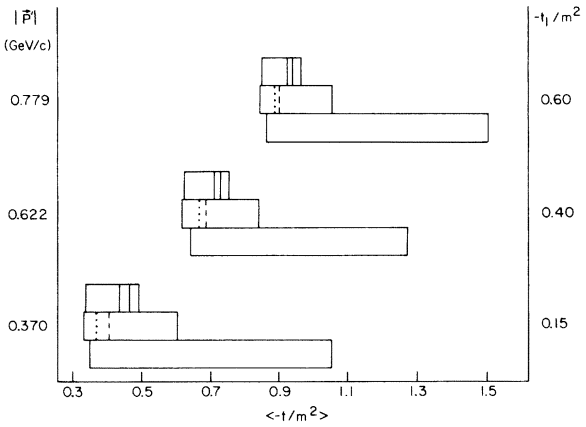

FIG. 6. Allowed ranges for $\langle -t/m^2 \rangle$ as a function of t_1 or $\vec{P}'^{\,min}$ for an incident neutrino beam characterized by the Argonne spectrum of Fig. 2 and Table I. For each value of t_1, the top, middle, and bottom bands correspond respectively to the WS model, an arbitrary V,A model, and to an arbitrary combination of S, P, and T. In the top band the right edge corresponds to $x=\sin^2\theta_W = 0$, the next vertical lines to $x=\frac{1}{4}$ and $x=\frac{1}{3}$, respectively, and the left edge to $x=x_{\min}\approx 0.6$. In the middle band the dotted and dashed lines correspond to a pure vector isoscalar current and a pure axial-vector current, respectively. It should be emphasized that no conclusions can be drawn from experiments with large values of t_1 because of the strong influence of unknown form factors. The bands with large t_1 in this figure have been included merely to illustrate the dependence of $\langle -t/m^2 \rangle$ on t_1 in the form-factor models we have considered. This same remark applies to the upper bands in Figs. 7–9 as well.

The vertical scale gives the experimental cut on the 3-momentum of the outgoing proton, or equivalently the value of $|t_1|$ in Eq. (2.1). We see from Fig. 5 that if $|t_1|$ is very small the V,A predictions for $\langle t \rangle$ fall into bands which do not overlap those for S,P. As expected $\langle -t^{S,P} \rangle$ is larger than $\langle -t^{V,A} \rangle$, and a clear distinction between the helicity-preserving and helicity-flipping cases is apparent. However, as $|t_1|$ increases the V,A band begins to merge with the S,P band, and at $|t_1| \approx 0.27m^2$ the distinction between the two begins to disappear.

This behavior reflects the fact that, although the S,P differential cross sections rise for small t, they turn over and fall, more or less as the V,A cross sections do, when the t dependence of the form factors begins to dominate that due to the interaction. Since the t dependence of $d\sigma^T/dt$ is similar to that of $d\sigma^{V,A}/dt$, inclusion of the tensor contribution would further blur the distinction between the helicity-preserving and helicity-flipping cases. This is another manifestation of the "confusion theorem."[10]

We turn next to the case where the incident neutrino beam is not monoenergetic. We define $\langle t \rangle$ to be the result obtained by computing $\langle t \rangle = [\sum tn(t)]/[\sum n(t)]$, where $n(t)$ is the number of events with momentum transfer t, *and any value of* s. We have determined the possible range of $\langle t \rangle$ values for each general type of interaction as a function of the experimental cut in t for this situation. Figures 6 and 7 give the results corresponding to the ANL and BNL spectra, respectively. In each figure, for each value of the cut in t, t_1, three horizontal bands are shown which correspond to the following cases: The top band gives the results for the Weinberg-Salam model with the internal lines denoting $x=\frac{1}{4}$ and $x=\frac{1}{3}$. The middle band corresponds to an arbitrary V,A model characterized by the three parameters $F_1(0)$, $F_2(0)$, and $G_1(0)$ defined in Eqs. (3.5). The maximum and minimum values of $\langle -t/m^2 \rangle$ in this band are obtained by extremizing the three-dimensional parameter space spanned by $F_1(0)$, $F_2(0)$, and $G_1(0)$. Also shown in this band are the results for the pure vector isoscalar current (dotted line) and the pure axial-vector current (dashed line). The lowest band in

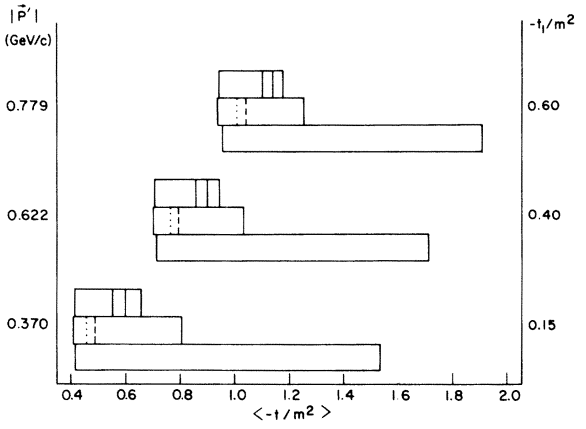

FIG. 7. Allowed ranges for $\langle -t/m^2 \rangle$ as a function of t_1 or $\vec{P}'^{\,\min}$ for an incident neutrino beam characterized by the Brookhaven spectrum of Fig. 3 and Table II. For details see text and caption to Fig. 6.

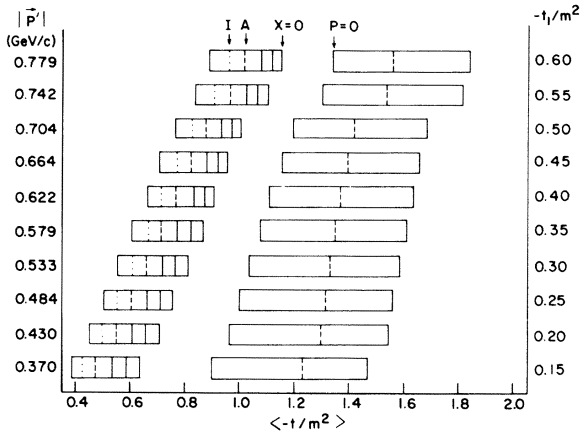

FIG. 8. $\langle -t/m^2 \rangle_w$ as a function of t_1 or $\vec{P}'^{\,\min}$ for an incident neutrino beam characterized by the Brookhaven spectrum. For each value of t_1 the left and right bands give the V,A and S,P predictions under the dynamical assumptions stated in the text. The arrows indicate the predictions for a pure vector isoscalar current (I), a pure axial-vector current (A), the Weinberg-Salam model with $x=0$, and a pure scalar current ($P=0$). For further details see text, and caption to Fig. 6.

each case gives the range of $\langle -t/m^2 \rangle$ for an arbitrary combination of S, P, and T characterized by the five parameters $S(0)$, $P(0)$, $T_1(0)$, $T_2(0)$, and $T_4(0)$. (We have assumed that $\mathfrak{M}^T_{\lambda\mu}$ contains only first-class currents.) The corresponding five-parameter space has been extremized with the extrema corresponding to the ends of the bands. We see from these results that an arbitrary V,A coupling can give rise to values of $\langle -t/m^2 \rangle$ that are not obtainable from the Weinberg-Salam model for any value of x. This is, of course, not surprising and indicates that a distinction among the V,A models themselves is possible based on a measurement of $\langle t \rangle$. We see from Fig. 7 that the results for the general V,A case can, in turn, be reproduced at BNL energies by an appropriate combination of S,T,P form factors, although the converse is not true.

In this connection it is useful to summarize the status of the "confusion theorem"[10] in νp and $\bar{\nu} p$ scattering. Recall that for $\nu_\mu e$ and $\bar{\nu}_\mu e$ scattering it was shown, assuming massless electrons, that for any admixture of V and A interactions, there is a corresponding admixture of S,P,T interactions which yields both the same $\nu_\mu e$ cross section and the same $\bar{\nu}_\mu e$ cross section. For νp and $\bar{\nu} p$ scattering the situation is as follows:

(i) For kinematic conditions under which m is not negligible, a $V \pm A$ coupling can be reproduced by an appropriate combination of S,P,T couplings, if we assume that all the proton form factors have a common t dependence. If all the proton form factors are retained, then $V \pm A$ is the only coupling which we know for certain can be confused with S,P,T: Other V,A couplings may also be subject to "confusion" but this question has not been settled to date.

(ii) If $m \neq 0$ and we set $F_1(t)$, $G_1(t)$, $T_1(t)$, $S(t)$, and $P(t)$ equal to constants, and all other form factors equal to zero, then we can rigorously show what *only* $V \pm A$ can be confused with S,P,T. This result has been noted earlier[10] for the case of massive electrons.

(iii) At very high energies, where we can safely set $m=0$, then any V,A theory can be confused with S,P,T, irrespective of which V,A form factors are included.

Even when a rigorous confusion theorem does not exist a "practical confusion theorem" may hold if a given set of data for $d\sigma^{\nu,\bar{\nu}}/dt$ can be fitted by both V,A and S,P,T models within the existing experimental errors. Examples of this have been discussed by Adler[13] for deep-inelastic neutrino scattering. When sufficiently good νp and $\bar{\nu} p$ data become available, it will then be appropriate to examine the "practical confusion theorem" in greater detail by attempting to fit the results with both V,A and S,P,T models.

When the number of observed events is sufficiently large, one can consider a more refined weighted average t. This is obtained by separating the events into bins of fixed s, computing $\langle t(s) \rangle$ for each bin, and then combining these bin averages, weighting each by the beam flux at the corresponding energy. The resulting average, which we denote by $\langle t \rangle_w$, may perhaps provide a more sensitive discriminator between different interactions. The $\langle t \rangle$ values which result from various interactions are shown in Figs. 8 and 9 for the

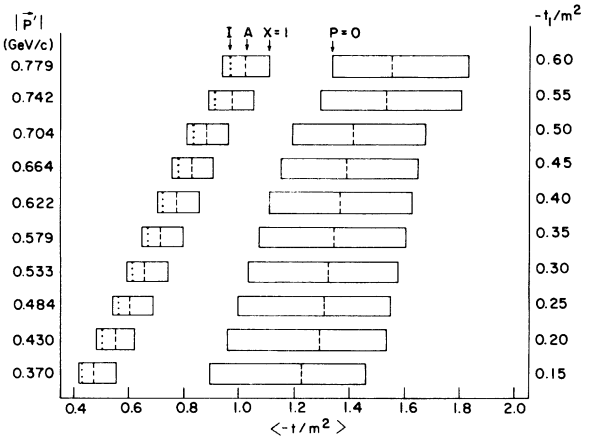

FIG. 9. $\langle -t/m^2 \rangle_w$ as a function of t_1 or $\vec{P}'^{\,\min}$ for an incident antineutrino beam characterized by the Brookhaven spectrum. We assume (as is approximately the case) that the ν and $\bar{\nu}$ spectra have the same shape albeit different normalizations. For further details see text and captions to Figs. 6 and 8.

Brookhaven neutrino and antineutrino beams, respectively. The V,A bands correspond to the Weinberg-Salam model with $x = \sin^2\theta_W$ ranging between 0 and 1. Although the maximum value of $\langle -t/m^2 \rangle_w$ is obtained for $x = 0$, the minimum corresponds not to $x = 1$ but to some other value which is usually in the vicinity of $x \approx \frac{2}{3}$. In Fig. 8 the two vertical lines in each V,A band correspond to the representative values $x = \frac{1}{4}$ and $x = \frac{1}{3}$, with the former value giving the higher result for $\langle -t/m^2 \rangle_w$. The dashed and dotted lines denoted by A and I in both figures correspond to a pure axial-vector and a pure vector isoscalar current, respectively, as discussed in Sec. III. In the S,P band the value of $\langle -t/m^2 \rangle_w$ depends on a single parameter, $|S(0)/P(0)|$, with the lower end of the band corresponding to $P(0) = 0$. The upper end, for which $S(0) = 0$, is given by either the solid vertical line or the dashed vertical line corresponding respectively to the dipole form or the pion dominance form for $P(t)$. The dipole form is assumed to be characterized by a mass $\Lambda = 0.9m$ in all of the V, A, S, and P form factors. We see from Figs. 8 and 9 that $\langle t \rangle_w$ distinguishes clearly between a V,A model of the Weinberg-Salam type and an arbitrary S,P coupling. However, the dependence of the observed t distribution and of $\langle t \rangle$ on the shape of unknown hadronic form factors must not be forgotten. We have tried to get some feeling for this dependence by varying the mass Λ in the dipole form. It was found that a 10% increase in Λ resulted in roughly a 10% increase in $\langle t \rangle_w$ when the other parameters were held constant.

To summarize this section, we have shown that $\langle t \rangle$ provides a crude distinction between V,A and S,P,T interactions. If the experimental results for $\langle -t/m^2 \rangle$ fall well outside the V,A bands then a clear signal for neutrino helicity-flip will be indicated. However, if a value of $\langle -t/m^2 \rangle$ in the V,A band is obtained, one can study $d\sigma/dt$ at Brookhaven for $|t| \lesssim 0.2$ (GeV/c)^2 to help rule out a dominant S,P term. Even if such a possibility is indeed ruled out, one has still not distinguished between V,A and S, P, *and* T. To accomplish this in νp or $\bar{\nu} p$ scattering would probably require a future generation of experiments, such as a measurement of the proton's polarization, to which we turn in the next section.

V. POLARIZATION PHENOMENA

If polarization measurements in νp scattering should ever become feasible, then one would expect rather striking polarizations, of the order of 100%, to be produced by some kinds of interactions. Furthermore, the polarizations resulting from V,A are quite different from those produced by S,P,T and so they ought to be very informative should the momentum-transfer data turn out to be compatible both with V,A and with S,P,T.

From angular momentum conservation alone, one can show that the polarizations observed at certain angles can give unambiguous evidence for the presence of certain kinds of couplings. For example, consider νp scattering at 0° in the center-of-mass (c.m.) frame. At this angle, a measured proton recoil polarization which is anything other than −100% in the neutrino-beam direction would prove that there is a V,A component in the neutral weak force. For, as shown in Fig. 10, if only the neutrino-helicity-flipping S, P, and T couplings are present, then at 0° the proton spin must flip in the opposite direction, so as to conserve angular momentum along the beam line. Thus, the incoming protons can interact only if their spins point in the neutrino-beam direction, and when they emerge, all their spins must point against it.

One may look for this behavior, or its absence, either by studying the dependence of the cross section on target polarization, or by measuring the polarization of the recoil protons. The latter approach is somewhat facilitated by the fact that longitudinal polarization of the protons in the c.m. frame would appear as *transverse* polarization in the lab. This makes it possible to measure the polarization by rescattering, and is due to the fact that protons suffering extremely small deflections in the c.m. frame emerge very near 90° to the beam in the lab. Of course, for precisely 0°, the proton has no recoil momentum at all, and so one must

ask to what extent the 100% polarization expected from Fig. 10 persists away from $t=0$. To explore this question, we have calculated the laboratory-frame polarizations produced by S,P,T and V,A interactions when the beam energy $Q_0 \ll m$. (The expressions applicable to the general case are given in the Appendix, but a discussion going beyond the simplest cases would seem premature at the present time.) When the neutrino energy is low, $|t_{\max}| \ll m^2$, and the proton recoil may be treated nonrelativistically, terms of order q/m in the proton matrix elements may be neglected, and the t dependence of most form factors may safely be ignored. For the S,P,T case, it is possible, in addition, to neglect the S,P amplitudes relative to those from T, so long as $\sqrt{-t} \ll (-t_{\max})^{1/2}$. (Recall that the S,P contributions vanish at $t=0$.) Thus, the "S,P,T" amplitudes may be taken to result from the T interaction

$$\mathcal{H} = \frac{G}{\sqrt{2}} \bar{\psi}_\nu \sigma_{\mu\alpha} \psi_\nu \bar{\psi}_p \sigma_{\mu\alpha} (\tau + \tilde{\tau}\gamma_5) \psi_p , \tag{5.1}$$

where τ and $\tilde{\tau}$ are effectively constants.[14] Similarly, the V,A amplitudes result from

$$\mathcal{H} = \frac{G}{\sqrt{2}} i\bar{\psi}_\nu \gamma_\mu (1+\gamma_5) \psi_\nu \, i\bar{\psi}_p \gamma_\mu (v - a\gamma_5) \psi_p , \tag{5.2}$$

where v and a are constants.

We denote the longitudinal polarization of the recoil proton in the laboratory frame by $\mathcal{P}_l$, and the transverse polarizations along $(\vec{Q}\times\vec{Q}')\times\vec{P}'$ and $\vec{Q}\times\vec{Q}'$ by $\mathcal{P}_t$ and $\mathcal{P}_n$, respectively. We express these in terms of the angles θ' and θ at which the neutrino and the proton, respectively, emerge in the laboratory relative to the beam direction. A beam of low-energy neutrinos, interacting via the tensor coupling (5.1), will produce recoil polarizations given by

$$\mathcal{P}_t^\nu = \frac{-2\sin(\theta + \frac{1}{2}\theta')\cos\frac{1}{2}\theta'}{1+\cos^2(\frac{1}{2}\theta')} , \tag{5.3a}$$

$$\mathcal{P}_l^\nu = \frac{-2\cos(\theta + \frac{1}{2}\theta')\cos\frac{1}{2}\theta'}{1+\cos^2(\frac{1}{2}\theta')} , \tag{5.3b}$$

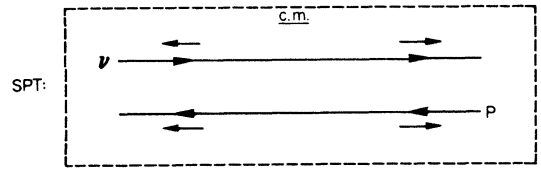

FIG. 10. Behavior of the neutrino and proton spins for 0° scattering in the center-of-mass frame, when only S, P, and T couplings are present. Note that the scattering of neutrinos off protons with initial + helicity via an S,P,T interaction is strictly forbidden by angular momentum conservation.

$$\mathcal{P}_n^\nu = 0 . \tag{5.3c}$$

For antineutrinos, each component of the polarization simply changes sign:

$$\vec{\mathcal{P}}^{\bar{\nu}} = -\vec{\mathcal{P}}^{\nu} . \tag{5.4}$$

If the coupling is V,A, Eq. (5.2), the polarizations produced by neutrinos are

$$\mathcal{P}_t^\nu = -2a \frac{v\sin(\theta+\frac{1}{2}\theta')\cos\frac{1}{2}\theta' - a\cos(\theta+\frac{1}{2}\theta')\sin\frac{1}{2}\theta'}{2a^2 + (v^2-a^2)\cos^2(\frac{1}{2}\theta')} , \tag{5.5a}$$

$$\mathcal{P}_l^\nu = -2a \frac{v\cos(\theta+\frac{1}{2}\theta')\cos\frac{1}{2}\theta' + a\sin(\theta+\frac{1}{2}\theta')\sin\frac{1}{2}\theta'}{2a^2 + (v^2-a^2)\cos^2(\frac{1}{2}\theta')} , \tag{5.5b}$$

$$\mathcal{P}_n^\nu = 0 . \tag{5.5c}$$

Antineutrinos will give polarizations related to these by

$$\vec{\mathcal{P}}^{\bar{\nu}}(a/v) = -\vec{\mathcal{P}}^{\nu}(-a/v) . \tag{5.6}$$

In Fig. 11 we have plotted the transverse polarization $\mathcal{P}_t^\nu$ versus $-t/m^2$ for the case of neutrinos with a laboratory energy $Q_0 = 0.05m$ (an energy characteristic of LAMPF, for example). We show the polarization which corresponds to pure T, Eq. (5.3a), and the special cases of the V,A polarization, Eq. (5.5a), which correspond to pure V, pure A, $V+A$, and $V-A$. One sees from Fig. 11 that over a considerable range in t, the polarization produced by the T interaction remains extremely close to the −100% required by Fig. 10 at $t=0$. This means that even for T accompanied by some S and P, the polarization will be close to −100% so long as $\sqrt{-t} \ll (-t_{\max})^{1/2}$.[15] We next ask how likely it is that a coupling involving a V,A component will yield something different. As illustrated in Fig. 11, most pure V,A combinations give polarizations which are very different from that due to S,P,T. Even for $V+A$, it is only for

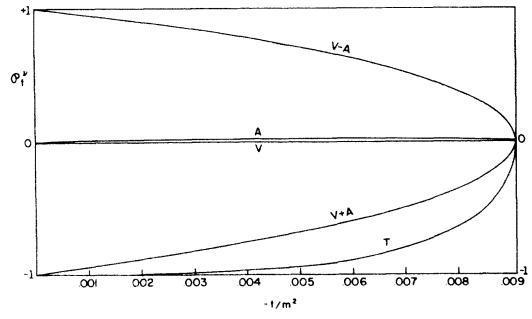

FIG. 11. The transverse polarization, along the direction $(\vec{Q}\times\vec{Q}')\times\vec{P}'$, produced by a neutrino beam with $Q_0(\text{lab}) = 0.05m$.

incident *neutrinos* that the polarization resembles that from S,P,T; for antineutrinos these two coupling schemes give large polarizations that differ in sign. Allowing for the possible simultaneous presence of S, P, V, A, and T, one finds that at $t=0$

$$\mathcal{P}_t^{\nu} = \frac{-2va - 2(|\tau|^2 + |\tilde{\tau}|^2)}{v^2 + a^2 + 2(|\tau|^2 + |\tilde{\tau}|^2)} \tag{5.7a}$$

and

$$\mathcal{P}_t^{\bar{\nu}} = \frac{-2va + 2(|\tau|^2 + |\tilde{\tau}|^2)}{v^2 + a^2 + 2(|\tau|^2 + |\tilde{\tau}|^2)} . \tag{5.7b}$$

These expressions show that, in principle at least, polarization measurements can always determine whether or not the interaction includes a V,A component.

VI. ELASTIC CROSS SECTIONS

Having already discussed what can be learned from the shape of the differential cross section in elastic neutrino-proton scattering, let us now see what can be learned from the overall rates for $\nu p \to \nu p$ and $\bar{\nu}p \to \bar{\nu}p$. Just as the weak-coupling constant, G, is determined by an analysis of muon decay in the case of charged-current interactions, the coupling strength of the weak neutral interactions, $\hat{G} = \lambda G$, is determined from experimental studies of the processes $\nu N \to \nu X$ and $\bar{\nu}N \to \bar{\nu}X$. This procedure was first employed by Adler and Tuan[16] and also by Sakurai and Urrutia[5] and we shall outline it here in some detail.

We begin by writing the neutral-current effective matrix element (for accelerator neutrinos) as[6,13,17]

$$\begin{aligned}\mathfrak{M}_{\text{eff}}^{\text{NC}} = \frac{G\lambda}{\sqrt{2}} \,[&\bar{\psi}_\nu(1+\gamma_5)\psi_\nu(\mathfrak{F}+\mathfrak{F}_5) \\ &+ \bar{\psi}_\nu(1+\gamma_5)\sigma_{\alpha\mu}\psi_\nu\mathfrak{F}_{\alpha\mu} \\ &+ \bar{\psi}_\nu\gamma_\mu(1+\gamma_5)\psi_\nu(\mathfrak{F}_\mu+\mathfrak{F}_{5\mu})] ,\end{aligned} \tag{6.1}$$

where λ is the parameter which characterizes the strength of the neutral-current interaction relative to that of the charged-current interaction. We also define the hadronic currents, $\mathfrak{F}$, as follows:

$$\mathfrak{F} = g_{S0}\mathfrak{F}^0 + g_{S3}\mathfrak{F}^3 + g_{S8}\mathfrak{F}^8 , \tag{6.2a}$$

$$\mathfrak{F}_5 = g_{P0}\mathfrak{F}_5^0 + g_{P3}\mathfrak{F}_5^3 + g_{P8}\mathfrak{F}_5^8 , \tag{6.2b}$$

$$\mathfrak{F}_\mu = g_{V0}\mathfrak{F}_\mu^0 + g_{V3}\mathfrak{F}_\mu^3 + g_{V8}\mathfrak{F}_\mu^8 , \tag{6.2c}$$

$$\mathfrak{F}_{5\mu} = g_{A0}\mathfrak{F}_{5\mu}^0 + g_{A3}\mathfrak{F}_{5\mu}^3 + g_{A8}\mathfrak{F}_{5\mu}^8 , \tag{6.2d}$$

$$\mathfrak{F}_{\alpha\mu} = g_{T0}\mathfrak{F}_{\alpha\mu}^0 + g_{T3}\mathfrak{F}_{\alpha\mu}^3 + g_{T8}\mathfrak{F}_{\alpha\mu}^8 , \tag{6.2e}$$

where $\mathfrak{F}^j$, $\mathfrak{F}_5^j$, $\mathfrak{F}_\lambda^j$, $\mathfrak{F}_{5\lambda}^j$, and $\mathfrak{F}_{\alpha\mu}^j$ are identified with the usual nonet of quark currents (q is the quark field),

$$\mathfrak{F}^j = \bar{q}\tfrac{1}{2}\lambda^j q , \tag{6.3a}$$

$$\mathfrak{F}_5^j = \bar{q}\gamma_5\tfrac{1}{2}\lambda^j q , \tag{6.3b}$$

$$\mathfrak{F}_\mu^j = \bar{q}\gamma_\mu\tfrac{1}{2}\lambda^j q , \tag{6.3c}$$

$$\mathfrak{F}_{5\mu}^j = \bar{q}\gamma_\mu\gamma_5\tfrac{1}{2}\lambda^j q , \tag{6.3d}$$

$$\mathfrak{F}_{\alpha\mu}^j = \bar{q}\sigma_{\alpha\mu}\tfrac{1}{2}\lambda^j q . \tag{6.3e}$$

To proceed we define the quantities

$$\begin{aligned} R_\nu &= \frac{\sigma(\nu N \to \nu X)}{\sigma(\nu N \to \mu^- X)} , \\ R_{\bar{\nu}} &= \frac{\sigma(\bar{\nu}N \to \bar{\nu}X)}{\sigma(\bar{\nu}N \to \mu^+ X)} . \end{aligned} \tag{6.4}$$

Using the form of the weak neutral current displayed in Eqs. (6.1) and (6.2) along with the assumptions of the quark-parton model, Adler obtains[6,13,17]

$$\begin{aligned} R_\nu + 3R_{\bar{\nu}} = \lambda^2\{&[g_{V0}(\tfrac{2}{3})^{1/2} + g_{V8}(\tfrac{1}{3})^{1/2}]^2 + g_{V3}{}^2 \\ &+ [g_{A0}(\tfrac{2}{3})^{1/2} + g_{A8}(\tfrac{1}{3})^{1/2}]^2 + (g_{A3})^2\} , \end{aligned} \tag{6.5}$$

for the case of an arbitrary combination of V and A, and

$$\begin{aligned} 3(R_\nu + R_{\bar{\nu}}) = \lambda^2\{&[\tfrac{1}{2}(\tfrac{2}{3})^{1/2}g_{S0} + \tfrac{1}{2}(\tfrac{1}{3})^{1/2}g_{S8}]^2 + (\tfrac{1}{2}g_{S3})^2 \\ &+ [\tfrac{1}{2}(\tfrac{2}{3})^{1/2}g_{P0} + \tfrac{1}{2}(\tfrac{1}{3})^{1/2}g_{P8}]^2 \\ &+ (\tfrac{1}{2}g_{P3})^2\} , \end{aligned} \tag{6.6}$$

for the S,P case.

It is straightforward to determine λ^2 for a given space-time structure of the neutral current using Eqs. (6.5) and (6.6) and the experimental values for R_ν and $R_{\bar{\nu}}$. We have taken these values from Refs. 5 and 16, and using these values we have computed the cross sections shown in Table III.[18] However, for the Weinberg-Salam model the overall strength of the neutral current is fixed once $x = \sin^2\theta_W$ is specified, and hence the corresponding cross sections have been computed directly without reference to the preceding normalization analysis.

From Table III we see that the experimental values $R_\nu = 0.23 \pm 0.09$[2] and 0.17 ± 0.05[3] fall within the range predicted by the WS model, but appear to be larger than the predictions of S,P models. This suggests that the neutral current is not predominantly S,P.

VII. CONCLUSIONS

We have considered what one can learn about the space-time structure of the neutral weak interaction from νp and $\bar{\nu}p$ elastic scattering. We have seen that it is relatively easy to rule out a pure S,P coupling. Indeed, the observed rate for νp elastic scattering, and the fact that the elastic $\bar{\nu}p$

TABLE III. Flux-averaged neutrino- and antineutrino-proton total cross sections, for the models defined in the text. The flux-averaged charged-current cross sections used in computing $R_\nu^{el}=\sigma(\nu p\to\nu p)/\sigma(\nu n\to\mu^- p)$ and $R_{\bar\nu}^{el}=\sigma(\bar\nu p\to\bar\nu p)/\sigma(\bar\nu p\to\mu^+ n)$ are $\sigma(\nu n\to\mu^- p)=3.02\times10^{-39}$ cm^2 and $\sigma(\bar\nu p\to\mu^+ n)=1.14\times10^{-39}$ cm^2.

Model	σ_ν (10^{-40} cm^2)	$\sigma_{\bar\nu}$ (10^{-40} cm^2)	R_ν^{el}	$R_{\bar\nu}^{el}$
Weinberg-Salam				
$x=0$	7.97	3.00	0.264	0.264
0.10	5.65	1.86	0.187	0.163
0.20	3.90	1.29	0.129	0.113
0.30	2.73	1.30	0.090	0.114
0.35	2.36	1.52	0.078	0.133
0.40	2.14	1.89	0.071	0.166
0.45	2.06	2.40	0.068	0.210
0.50	2.13	3.06	0.070	0.268
0.60	2.70	4.80	0.089	0.421
0.70	3.85	7.13	0.127	0.625
0.80	5.58	10.04	0.185	0.880
0.90	7.88	13.53	0.261	1.186
1.00	10.77	17.60	0.356	1.543
$\mathcal{F}_\lambda^3+\mathcal{F}_{5\lambda}^3$	3.19	1.20	0.105	0.105
$\mathcal{F}_\lambda^8+\mathcal{F}_{5\lambda}^8$	1.50	1.09	0.050	0.096
$\mathcal{F}_\lambda^3+\frac{1}{\sqrt{3}}\mathcal{F}_\lambda^8+\mathcal{F}_{5\lambda}^3+\frac{1}{\sqrt{3}}\mathcal{F}_{5\lambda}^8$	5.15	2.31	0.170	0.203
$\mathcal{F}_\lambda^3+\frac{1}{\sqrt{3}}\mathcal{F}_\lambda^8$	5.21	5.21	0.172	0.457
$\mathcal{F}_\lambda^0$ [a]	5.46	5.46	0.181	0.478
$\mathcal{F}_{5\lambda}^8$	0.478	0.478	0.016	0.042
$\mathcal{F}_{5\lambda}^3$	1.38	1.38	0.046	0.121
$\mathcal{F}_\lambda^8$	2.06	2.06	0.068	0.182
$\mathcal{F}^8+\mathcal{F}_5^8$	1.57	1.57	0.052	0.138
$\mathcal{F}^3+\mathcal{F}_5^3$	0.146	0.146	0.005	0.013
$\mathcal{F}^0+\mathcal{F}_5^0$	1.57	1.57	0.052	0.137
$\mathcal{F}^3$	0.269	0.269	0.009	0.024
$\mathcal{F}_5^3$ [b]	1.95	1.95	0.064	0.171
$\mathcal{F}_5^8$	0.702	0.702	0.023	0.062
$\mathcal{F}^8$	2.44	2.44	0.080	0.214
$\mathcal{F}^0$	2.44	2.44	0.080	0.214
$\mathcal{F}_5^0$	0.702	0.702	0.023	0.062
$\mathcal{F}_5^3+\mathcal{F}_5^8$ [b]	2.65	2.65	0.087	0.232
$\mathcal{F}_5^0+\mathcal{F}_5^8$	0.702	0.702	0.023	0.062
$\mathcal{F}^3+\mathcal{F}^8+\mathcal{F}_5^3+\mathcal{F}_5^8$ [b]	2.08	2.08	0.068	0.182
$\mathcal{F}^3+\mathcal{F}^8$	1.51	1.51	0.050	0.132
$\mathcal{F}_5^3$	0.022	0.022	0.001	0.002

[a] We have used the fermion-current model of Sakurai (Ref. 7).
[b] A dipole form factor was assumed for $\mathcal{F}_5^3$ in this case.

and νp cross sections differ, already appear to accomplish this. Further νp measurements that would confirm this conclusion have been indicated.

By contrast, in νp elastic scattering it is very difficult to distinguish between a combination of S, P, *and* T on the one hand, and some admixture of V and A on the other, as we discussed in Sec. IV. Nevertheless, one can ask whether the shape of the t distribution, and correspondingly the average value of t, are *consistent* with a V,A interaction. If they are, one can attempt to determine the details of the coupling (the Weinberg angle, for example), although such an attempt is complicated by our uncertain knowledge of the hadronic form factors which are involved.

In closing, we comment briefly on the evidence concerning the space-time structure of the neutral weak force from other reactions. Table IV presents a summary of the processes which have been considered to date as probes of the neutral weak current.[1-6,10,13,16,17,19-32] Some of these are similar in nature to those considered earlier in the study of the charged weak current.[33,34] Evidence that the coupling is not dominantly S,P has come from the y distributions in high-energy inclusive scattering,[35] and very recently from the angular distribution for the process $\nu n \to \nu p \pi^-$.[36] That the neutral interaction is V and A, and not some combination of S, P, *and* T, is very much harder to show in neutrino reactions on nucleon or electron targets. Neutrino experiments with nuclear targets[10,31] and measurements in e^+e^- collisions[37] are potential sources of clean information on this issue. The scattering of *electron-type* neutrinos from electrons is also a possible source of insight, because of its sensitivity to interference between charged- and neutral-current effects.[10] For example, if the $\nu_e e^-$ cross section is less than the value expected (from μ decay) for the charged-current interaction acting alone, then the neutral current of the electron must contain a $V-A$ piece. Finally, we note that the observation of parity violation in an atom, at a level corresponding to a weak coupling of order G_F, the Fermi coupling constant, would imply the presence of a $V\times A$ neutral weak interaction of this strength. Parity-violating S,P,T atomic weak interactions have already been shown to be at least one thousand times weaker than this by using the limits on the electric dipole moments of certain atoms and molecules.[38] Furthermore, because of their phase, parity-odd S,P,T amplitudes cannot interfere with the electromagnetic amplitudes to produce the parity-violating effects for which one is looking.[39]

ACKNOWLEDGMENTS

The authors are indebted to M. Levine and J. Missimer for checking Eq. (A1) by use of Professor Levine's symbolic program ASHMEDAI. We wish to thank D. D. Carmony and L. Sulak for supplying us with the Argonne and Brookhaven spectra respectively and, along with V. E. Barnes, A. Garfinkel, and J. Smith, for helpful discussions. Two of us (B.K. and S.P.R.) wish to acknowledge the hospitality of CERN where part of this work was carried out.

APPENDIX: DIFFERENTIAL CROSS SECTION AND POLARIZATION FORMULAS

In this Appendix we give the detailed expressions for the νp and $\bar{\nu} p$ differential cross sections and for the polarization of the outgoing proton. These can be obtained from Eqs. (3.5) and (3.7) by use of standard techniques. The necessary trace calculations were executed with the aid of SCHOONSCHIP (a CDC 6600 program, written by M. Veltman, for symbolic evaluation of algebraic expressions), and checked against the results of ASHMEDAI, written by M. Levine. In order to facilitate the comparison of our results to those

TABLE IV. Summary of hadronic probes of the neutral current. A × indicates the current component to which the given experiment is sensitive.

Experiment	V	A	S	P	T	Isovector	Isoscalar	References
$\nu+p\to\nu+p$	×	×	×	×	×	×	×	1–6, 13, 16, 17, 19–21
$\nu+N\to\nu+N+\pi$	×	×	×	×	×	×	×	6, 13, 16, 17, 22, 23
$\nu+N\to\nu+X$	×	×	×	×	×	×	×	6, 10, 13, 16, 17, 22, 24–28
$\nu(\bar{\nu})+d\to\nu(\bar{\nu})+d$	×	×	×	×	×		×	29
$\nu+{}^4\mathrm{He}\to\nu+{}^4\mathrm{He}$	×		×				×	10
$\nu+{}^{12}\mathrm{C}\to\nu+{}^{12}\mathrm{C}(15.11\ \mathrm{MeV})$		×			×	×		10, 30
$\nu+\text{nucleus}\to\nu+\text{nucleus}+1^{\pm}\ \text{meson}$	×	×				×	×	31
$\pi^0\to\nu\bar{\nu}$				×		×		10, 32
$\eta\to\nu\bar{\nu}$				×			×	32

of Adler *et al.*[6] we let the form factors appearing in Eqs. (3.5) and (3.7) be arbitrary complex functions of the momentum transfer t. We then have

$$\begin{aligned}\frac{-8\pi(s-m^2)^2}{G^2}\frac{d\sigma^{\nu,\bar\nu}}{dt} = {} & S|^2 t(t-4m^2)+|P|^2t^2+|T_1|^2 8[4(s-m^2)^2+t(4s+t-2m^2)] \\ & -|T_2|^2\frac{16t}{m^2}(s-m^2)(s-m^2+t)-|T_3|^2\frac{16t}{m^2}[(s-m^2)^2+st] \\ & +|T_4|^2\frac{4t}{m^4}\{-16m^2(s-m^2)^2+t[(2s+t)^2-4m^2(6s+2t-5m^2)]\} \\ & -4t[2(s-m^2)+t][\pm 2\,\mathrm{Re}(ST_2^*)\mp\mathrm{Re}(PT_1^*)\mp\mathrm{Re}(ST_1^*)] \\ & \pm\mathrm{Re}(ST_4^*)\frac{4t}{m^2}[-8m^2(s-m^2)+t(t+2s-6m^2)]-16t^2\mathrm{Re}(T_1T_2^*) \\ & +\frac{8t}{m^2}[4(s-m^2)^2+t(-4m^2+4s+t)][\mathrm{Re}(T_1T_4^*)-2\,\mathrm{Re}(T_2T_4^*)] \\ & +2(|F_1|^2+|G_1|^2)[2(s-m^2)^2+t(t+2s)]-|F_2|^2\frac{t}{m^2}[(s-m^2)^2+t(s-2m^2)] \\ & -8|G_1|^2m^2t\mp 4[\mathrm{Re}(F_1G_1^*)+\mathrm{Re}(F_2G_1^*)]t[t+2(s-m^2)] \\ & +4\,\mathrm{Re}(F_1F_2^*)t^2-|G_2|^2\frac{t}{m^2}[(s-m^2)^2+st]. \end{aligned} \tag{A1}$$

The upper and lower signs in (A1) correspond to ν and $\bar\nu$, respectively. For the purpose of calculating $\langle t\rangle$ it is convenient to express the differential cross sections $d\sigma^\pm/dt$ (corresponding to $+=V,A$ and $-=S,P,T$) in the form

$$\frac{d\sigma^\pm}{dt}=-\frac{G^2}{8\pi}\frac{1}{(s-m^2)^2}\sum_{n=0}^{4}R_n^\pm(s,t)t^n\,, \tag{A2}$$

in which the coefficients $R_n^\pm(s,t)$ of each power n of t in Eq. (A1) are exhibited explicitly. The t dependence of $R_n^\pm(s,t)$ then arises solely from the form factors $F_1(t)$, $G_1(t),\ldots$, etc. If we factor out the assumed t dependence of the form factors as in Eq. (3.18), $d\sigma^\pm/dt$ can then be expressed in terms of the functions $R_n^\pm(s,0)\equiv R_n^\pm(s)$ in which the expressions F_1, $G_1,\ldots$ mean $F_1(0)$, $G_1(0),\ldots$, etc. The coefficients $R_n^\pm(s)$ then determine $\langle t(s)\rangle$ through Eq. (4.3). We have

$$R_0^+(s)=4(s-m^2)^2(|F_1|^2+|G_1|^2)\,, \tag{A3a}$$

$$\begin{aligned}R_1^+(s)= {} & \mp 8(s-m^2)[\mathrm{Re}(F_1G_1^*)+\mathrm{Re}(F_2G_1^*)]+4s(|F_1|^2+|G_1|^2) \\ & -\frac{(s-m^2)^2}{m^2}(|F_2|^2+|G_2|^2)-8m^2|G_1|^2\,,\end{aligned} \tag{A3b}$$

$$R_2^+(s)=2[|F_1|^2+|G_1|^2\mp 2\,\mathrm{Re}(F_1G_1^*)]\mp 4\,\mathrm{Re}(F_2G_1^*)+4\,\mathrm{Re}(F_1F_2^*)-\frac{(s-2m^2)}{m^2}|F_2|^2-\frac{s}{m^2}|G_2|^2\,, \tag{A3c}$$

$$R_0^-(s)=32(s-m^2)^2|T_1|^2\,, \tag{A3d}$$

$$\begin{aligned}R_1^-(s)= {} & -4m^2|S|^2+16(2s-m^2)|T_1|^2-\frac{16(s-m^2)^2}{m^2}(|T_2|^2+|T_3|^2+4|T_4|^2) \\ & -8(s-m^2)[\pm 2\,\mathrm{Re}(ST_2^*)\mp\mathrm{Re}(PT_1^*)\mp\mathrm{Re}(ST_1^*)]\mp 32(s-m^2)\,\mathrm{Re}(ST_4^*) \\ & +32\frac{(s-m^2)^2}{m^2}[\mathrm{Re}(T_1T_4^*)-2\,\mathrm{Re}(T_2T_4^*)]\,,\end{aligned} \tag{A3e}$$

$$\begin{aligned}R_2^-(s)= {} & |S|^2+|P|^2+8|T_1|^2-\frac{16(s-m^2)}{m^2}|T_2|^2-\frac{16s}{m^2}|T_3|^2 \\ & +\frac{16}{m^4}(s-m^2)(s-5m^2)|T_4|^2-4[\pm 2\,\mathrm{Re}(ST_2^*)\mp\mathrm{Re}(PT_1^*)\mp\mathrm{Re}(ST_1^*)] \\ & \pm\frac{8}{m^2}(s-3m^2)\,\mathrm{Re}(ST_4^*)-16\,\mathrm{Re}(T_1T_2^*)+32\frac{(s-m^2)}{m^2}[\mathrm{Re}(T_1T_4^*)-2\,\mathrm{Re}(T_2T_4^*)]\,,\end{aligned} \tag{A3f}$$

$$R_3^-(s) = \frac{16}{m^4}(s-2m^2)|T_4|^2 \pm \frac{4}{m^2}\,\mathrm{Re}(ST_4^*) + \frac{8}{m^2}\left[\mathrm{Re}(T_1T_4^*) - 2\,\mathrm{Re}(T_2T_4^*)\right], \tag{A3g}$$

$$R_4^-(s) = \frac{4}{m^4}|T_4|^2. \tag{A3h}$$

We turn next to the polarization $\mathcal{P}$ which we define as follows:

$$\mathcal{P} = \frac{d\sigma^+(w)/dt - d\sigma^-(w)/dt}{d\sigma^+(w)/dt + d\sigma^-(w)/dt}. \tag{A4}$$

$d\sigma^\pm(w)/dt$ are the differential cross sections for producing a proton with spin pointing along $\pm\hat{w}$, where $\hat{w}$ is an arbitrary direction. For longitudinal proton polarization $w_\lambda^{(\mathrm{long})}$ is given by

$$w_\lambda^{(\mathrm{long})} = (\vec{w}^{(\mathrm{long})}, w_4^{(\mathrm{long})}) = \left(\frac{P_0'\hat{P}'}{m},\ i\,\frac{|\vec{P}'|}{m}\right), \tag{A5}$$

while a transversely polarized proton is described by

$$w_\lambda^{(\mathrm{trans})} = (\hat{n}, 0), \tag{A6}$$

where $\hat{n}$ is a unit vector transverse to the proton 3-momentum, i.e., $\hat{n}\cdot\vec{P}' = 0$. For other polarization directions w_λ can be appropriately defined subject to the transversality condition

$$w_\lambda P_\lambda' = 0. \tag{A7}$$

In what follows we quote the general polarization formulas for V, A and S, T, P in the form

$$\mathcal{P} = \mathcal{P}_{\mathrm{in}} + \mathcal{P}_{\mathrm{out}}, \tag{A8}$$

where $\mathcal{P}_{\mathrm{in,\,out}}$ correspond respectively to polarizations in and out of the scattering plane. In each case the upper (lower) sign describes ν ($\bar{\nu}$). We have

$$\begin{aligned}
\mathcal{P}_{\mathrm{in}}(V,A) = \frac{m}{B}\{&\mp 4m^2t|F_1|^2 \mp t\,\mathrm{Re}(F_1F_2^*)(t+4m^2) + 8m^2\,\mathrm{Re}(F_1G_1^*)(s-m^2)\\
&+ t[2(s-m^2)+t][\mathrm{Re}(F_1G_2^*) + \mathrm{Re}(F_2G_2^*)] \mp t^2|F_2|^2\\
&+ t\,\mathrm{Re}(F_2G_1^*)(2s+t) \mp t\,\mathrm{Re}(G_1G_2^*)(t-4m^2)\}(Q+Q')\cdot w\\
&\mp \frac{4m^3}{B}[2(s-m^2)+t]|G_1|^2(Q-Q')\cdot w + \frac{m^3t}{B}[8\,\mathrm{Re}(F_1G_1^*) + 2\,\mathrm{Re}(F_2G_1^*)]\,Q\cdot w - \frac{6m^3}{B}\,\mathrm{Re}(F_2G_1^*)t\,Q'\cdot w\\
&+ \frac{m}{B}\{\mp t[2(s-m^2)+t][\mathrm{Re}(F_1F_2^*) + \mathrm{Re}(G_1G_2^*) + |F_2|^2] + t^2\mathrm{Re}(F_2G_2^*) + 4m^2t\,\mathrm{Re}(F_1G_2^*)\\
&\quad + [4(s-m^2)^2 + 4t(s-m^2) + t^2][\mathrm{Re}(F_2G_1^*) + \mathrm{Re}(F_1G_2^*)]\}P\cdot w,
\end{aligned} \tag{A9a}$$

$$\begin{aligned}
\mathcal{P}_{\mathrm{out}}(V,A) = &\pm\frac{2i}{B}\epsilon_{\alpha\beta\gamma\delta}w_\alpha Q_\beta' P_\gamma Q_\delta\{-2mt[\mathrm{Im}(F_1G_2^*) + \mathrm{Im}(F_2G_2^*) - \mathrm{Im}(F_2G_1^*)] + 8m^3\mathrm{Im}(F_1G_1^*)\}\\
&+\frac{2i}{B}\epsilon_{\alpha\beta\gamma\delta}w_\alpha P_\beta' P_\gamma Q_\delta\{-2m[2(s-m^2)+t][\mathrm{Im}(F_1F_2^*) + \mathrm{Im}(G_1G_2^*)]\},
\end{aligned} \tag{A9b}$$

$$\begin{aligned}
B = &\,2m^2(|F_1|^2 + |G_1|^2)[2(s-m^2)^2 + t(2s+t)] - 8m^4t|G_1|^2\\
&+ 4m^2t^2\mathrm{Re}(F_1F_2^*) \mp 4m^2t[\mathrm{Re}(F_1G_1^*) + \mathrm{Re}(F_2G_1^*)][2(s-m^2)+t]\\
&- t|G_2|^2[(s-m^2)^2 + st] - t|F_2|^2[(s-m^2)(s-m^2+t) - m^2t],
\end{aligned} \tag{A9c}$$

$$\mathcal{P}_{\text{in}}(S,P,T)=\pm\frac{4}{A}\{8m^4|T_1|^2(m^2-s)+4m^2t[s\,\mathrm{Re}(T_1T_2^*)+s\,\mathrm{Im}(T_1T_3^*)-\mathrm{Im}(T_2T_3^*)(2(s-m^2)+t)]$$
$$-2t\,\mathrm{Im}(T_3T_4^*)[-8m^2(s-m^2)+t(2s+t-6m^2)]\pm m^2t(t-4m^2)\mathrm{Im}(ST_3^*)$$
$$\mp 2m^4t\,\mathrm{Re}(PT_1^*)\pm m^2t^2\,\mathrm{Re}(PT_2^*)\}(Q+Q')\cdot w$$
$$\pm\frac{4}{A}\{4m^2t(4m^2-t)\mathrm{Re}(T_1T_4^*)\mp 2m^4[2(s-m^2)+t]\,\mathrm{Re}(ST_1^*)\}(Q-Q')\cdot w$$
$$\pm\frac{4}{A}\{-8m^4t|T_1|^2+4m^2t[\mathrm{Re}(T_1T_2^*)(t+m^2)+\mathrm{Im}(T_1T_3^*)(t-3m^2)]\}Q\cdot w$$
$$\pm\frac{16m^4t}{A}[\mathrm{Im}(T_1T_3^*)-3\,\mathrm{Re}(T_1T_2^*)]Q'\cdot w$$
$$\pm\frac{4}{A}\{-4m^4t[|T_1|^2+2\,\mathrm{Im}(T_1T_3^*)]+16m^2\mathrm{Re}(T_1T_4^*)[(s-m^2)^2+st]$$
$$+4m^2[(s+t)^2+(s-2m^2)^2-2m^4][\mathrm{Re}(T_1T_2^*)+\mathrm{Im}(T_1T_3^*)]$$
$$-4m^2t^2\mathrm{Im}(T_2T_3^*)-2t\,\mathrm{Im}(T_3T_4^*)[4(s-m^2)^2+t(4s+t-4m^2)]$$
$$+m^2t[2(s-m^2)+t][\pm\,\mathrm{Re}(PT_2^*)\pm\mathrm{Im}(ST_3^*)\pm 2\,\mathrm{Re}(PT_4^*)]-m^4t\,\mathrm{Re}(SP^*)\}P\cdot w, \tag{A10a}$$

$$\mathcal{P}_{\text{out}}(S,P,T)=\frac{8i}{A}\epsilon_{\alpha\beta\gamma\delta}w_\alpha Q'_\beta P_\gamma Q_\delta[\pm 2m^2t\,\mathrm{Re}(PT_3^*)\pm 4m^4\mathrm{Im}(ST_1^*)]$$
$$+\frac{8i}{A}\epsilon_{\alpha\beta\gamma\delta}w_\alpha P'_\beta P_\gamma Q_\delta\{\pm 2m^2t\,\mathrm{Im}(ST_2^*)+8m^2\,\mathrm{Im}(T_1T_4^*)[2(s-m^2)+t]$$
$$+8m^2[\mathrm{Im}(T_1T_2^*)-\mathrm{Re}(T_1T_3^*)](s-m^2)+4m^2t[\mathrm{Im}(T_1T_2^*)-\mathrm{Re}(T_1T_3^*)]$$
$$-4t\,\mathrm{Im}(T_2T_4^*)[2(s-m^2)+t]\}, \tag{A10b}$$

$$A=|S|^2m^3t(t-4m^2)+|P|^2m^3t^2+|T_1|^28m^3[4(s-m^2)^2+t(4s+t-2m^2)]$$
$$-|T_2|^216mt(s-m^2)(s-m^2+t)-|T_3|^216mt[(s-m^2)^2+st]$$
$$+|T_4|^2\frac{4t}{m}\{-16m^2(s-m^2)^2+t[(2s+t)^2-4m^2(6s+2t-5m^2)]\}$$
$$-4m^3t[2(s-m^2)+t][\pm 2\,\mathrm{Re}(ST_2^*)\mp\mathrm{Re}(PT_1^*)\mp\mathrm{Re}(ST_1^*)]$$
$$\pm\mathrm{Re}(ST_4^*)4mt[-8m^2(s-m^2)+t(t+2s-6m^2)]-16m^3t^2\,\mathrm{Re}(T_1T_2^*)$$
$$+8mt[4(s-m^2)^2+t(-4m^2+4s+t)][\mathrm{Re}(T_1T_4^*)-2\,\mathrm{Re}(T_2T_4^*)]\,. \tag{A10c}$$

---

*Work supported in part by the United States Energy Research and Development Administration.

[1]E. Fischbach, J. T. Gruenwald, S. P. Rosen, H. Spivack, and B. Kayser, Phys. Rev. Lett. 37, 582 (1976). Some typographical errors in Eqs. (1) and (2) of this reference are corrected in the present paper.

[2]W. Lee, E. Maddry, W. Sippach, P. Sokolsky, L. Teig, A. Bross, T. Chapin, L. Nodulman, T. O'Halloran, C. Y. Pang, K. Goulianos, and L. Litt, Phys. Rev. Lett. 37, 186 (1976).

[3]D. Cline, A. Entenberg, W. Kozanecki, A. K. Mann, D. D. Reeder, C. Rubbia, J. Strait, L. Sulak, and H. H. Williams, Phys. Rev. Lett. 37, 252 (1976).

[4]D. Cline, A. Entenberg, W. Kozanecki. A. K. Mann, D. D. Reeder, C. Rubbia, J. Strait, L. Sulak, and H. H. Williams, Phys. Rev. Lett. 37, 648 (1976).

[5]J. J. Sakurai and L. F. Urrutia, Phys. Rev. D 11, 159 (1975).

[6]S. L. Adler, E. W. Colglazier, Jr., J. B. Healy, I. Karliner, J. Lieberman, Y. J. Ng, and H.-S. Tsao, Phys. Rev. D 12, 3501 (1975); 11, 3309 (1975).

[7]H. Fritzsch, M. Gell-Mann, and P. Minkowski, Phys. Lett. 59B, 256 (1975); M. A. B. Bég and A. Zee, Phys. Rev. Lett. 30, 675 (1973); J. J. Sakurai, Phys. Rev. D 9, 250 (1974).

[8]D. D. Carmony (private communication); M. Derrick, in *Proceedings of the Sixth International Symposium on Electron and Photon Interactions at High Energies*, Bonn, 1973 (North-Holland, Amsterdam, 1974), p. 369.

[9]L. Sulak (private communication).

[10]B. Kayser, G. T. Garvey, E. Fischbach, and S. P. Rosen, Phys. Lett. 52B, 385 (1974).

[11]A. Salam and J. C. Ward, Phys. Lett. 13, 168 (1964); S. Weinberg, Phys. Rev. Lett. 19, 1264 (1967).

[12]B. W. Lee, summary talk at International Neutrino Conference 1976, Aachen, W. Germany (unpublished).

[13]S. L. Adler, in *Proceedings of the Sixth Hawii Topical Conference in Particle Physics, 1975*, edited by P. N. Dobson, Jr., S. Pakvasa, V. Z. Peterson, and S. F. Tuan (Univ. Press of Hawaii, Honolulu, 1976), p. 141.

[14]The negligible terms in the tensor matrix element include those of the form $(1/m)\bar{u}_p(\gamma_\mu Q_\nu - \gamma_\nu Q_\mu)u_p$. In this expression Q_ν/m is large in the lab frame only when $\nu=4$, but then it is multiplied by $\bar{u}_p\gamma_\mu u_p$ with $\mu=1$, 2, or 3 and this is of order $\vec{P}'/m$.

[15]A *pure* S,P interaction produces zero polarization (at low energies), avoiding the constraint of Fig. 10 by giving a vanishing rate at 0°. However, given the evidence against pure S,P, this is not the case of interest here. At higher energies, pure S,P produces nonzero polarizations which are, however, confined to the scattering plane, as can be seen from Eqs. (A10).

[16]S. L. Adler and S. F. Tuan, Phys. Rev. D 11, 129 (1975).

[17]S. L. Adler, Phys. Rev. D 12, 2644 (1975).

[18]In Table III, as well as in Table I of Ref. 1, we have assumed that the Sachs form factors $G_{E,M}$ rather than the Pauli form factors $F_{1,2}$ are characterized by the dipole t dependence of Eq. (3.18). This has been done to make our t dependence conform to that assumed by other authors in analyzing the data of Refs. 1 and 2. For the kinematic region where $\langle t\rangle$ can distinguish between V,A and S,P,T both sets of vector form factors give essentially the same results.

[19]F. Martin, Nucl. Phys. B104, 111 (1976).

[20]C. H. Albright, C. Quigg, R. E. Schrock, and J. Smith, Phys. Rev. D 14, 1780 (1976); V. Barger and D. V. Nanopoulos, Phys. Lett. 63B, 168 (1976).

[21]D. P. Sidhu, Brookhaven Report No. BNL-21468, (unpublished); Phys. Rev. D 14, 2235 (1976); R. M. Barnett, *ibid.* 14, 2990 (1976).

[22]R. L. Kingsley, F. Wilczek, and A. Zee, Phys. Rev. D 10, 2216 (1974).

[23]G. Branco, T. Hagiwara, and R. Mohapatra, Phys. Rev. Lett. 34, 703 (1975).

[24]S. Pakvasa and G. Rajasekaran, Phys. Rev. D 12, 113 (1975).

[25]M. Gronau and N. Levy, Nucl. Phys. B97, 513 (1975).

[26]J. Bell and G. Dass, Phys. Lett. 59B, 343 (1975).

[27]M. Gronau, Lett. Nuovo Cimento 14, 204 (1975).

[28]G. Ecker, Nucl. Phys. B107, 481 (1976).

[29]A. Pais and S. B. Treiman, Phys. Rev. D 9, 1459 (1974).

[30]T. Donnelly, D. Hitlin, M. Schwartz, J. Walecka, and S. Wiesner, Phys. Lett. 49B, 8 (1974).

[31]M. Gaillard, S. Jackson, and D. Nanopoulos, Nucl. Phys. B102, 326 (1976); R. Brown, L. Gordon, J. Smith, and K. Mikaelian, Phys. Rev. D 13, 1856 (1976); M. Einhorn and B. Lee, *ibid.* 13, 43 (1976); J. Pumplin and W. Repko, *ibid.* 12, 1376 (1975).

[32]E. Fischbach, J. T. Gruenwald, S. P. Rosen, H. Spivack, A. Halprin, and B. Kayser, Phys. Rev. D 13, 1523 (1976).

[33]C. Jarlskog, Lett. Nuovo Cimento 4, 377 (1970).

[34]T. P. Cheng and W.-K. Tung, Phys. Rev. D 3, 733 (1971).

[35]B. Barish *et al.*, in *La Physique du Neutrino à Haute Énergie*, Proceedings of the Colloquium, Paris, 1975 (CNRS, Paris, 1975).

[36]For pure S,P the distribution in the c.m. neutrino scattering angle θ must go like $\sin^2(\frac{1}{2}\theta)$ near the forward direction. At the International Neutrino Conference, Aachen, W. Germany, 1976 (unpublished), P. Schreiner reported data from an Argonne-Purdue collaboration which are inconsistent with this behavior.

[37]B. Kayser, S. P. Rosen, and E. Fischbach, Phys. Rev. D 11, 2547 (1975).

[38]C. Bouchiat, Phys. Lett. 57B, 284 (1975); E. Hinds, C. Loving, and P. Sandars, *ibid.* 62B, 97 (1976).

[39]C. Jarlskog (private communication).